# Magnetic behavior and chaining of strontium ferrite-nylon composite above the melting temperature

Cite as: AIP Advances 13, 025024 (2023); https://doi.org/10.1063/9.0000596 Submitted: 03 October 2022 • Accepted: 12 January 2023 • Published Online: 07 February 2023

🗓 Tanjina N. Ahmed, 🗓 Christopher Selsor, 🗓 Jitendra S. Tate, et al.

### **COLLECTIONS**

Paper published as part of the special topic on 67th Annual Conference on Magnetism and Magnetic Materials









v Online Export Citat





# Magnetic behavior and chaining of strontium ferrite-nylon composite above the melting temperature

Cite as: AIP Advances 13, 025024 (2023); doi: 10.1063/9.0000596 Submitted: 3 October 2022 • Accepted: 12 January 2023 • **Published Online: 7 February 2023** 













Tanjina N. Ahmed. 1.41 📵 Christopher Selsor, 2 📵 Jitendra S. Tate, 1.5 📵 and Wilhelmus J. Geerts 1.4 📵



## **AFFILIATIONS**

- <sup>1</sup> Materials Science, Engineering, and Commercialization, Texas State University, San Marcos, Texas 78666, USA
- <sup>2</sup>Aerospace Engineering, Texas A & M University, College Station, Texas 77843, USA
- Mechanical and Manufacturing Engineering, Texas State University, San Marcos, Texas 78666, USA
- Department of Physics, Texas State University, San Marcos, Texas 78666, USA

Note: This paper was presented at the 67th Annual Conference on Magnetism and Magnetic Materials.

a) Author to whom correspondence should be addressed: tna30@txstate.edu

#### **ABSTRACT**

To better understand Magnetic Field Assisted Additive Manufacturing (MFAAM) the effect of a magnetic field on the orientation and distribution of magnetic particles in a molten magnetic composite was studied. Vibrating Sample Magnetometer (VSM) measurements were made on Sr-ferrite/PA12 fused deposition modeling filaments of different packing fraction (5 and 40 wt. %). The rotation of the sample's magnetic moment upon application of a field perpendicular to the easy axis was monitored with a biaxial VSM above the PA12's softening temperature. The observed magnetic moment transients depend on the temperature, the applied alignment field, the packing fraction, and the initial field-anneal procedure. Longer field-anneals result in larger time constants and seem to induce a hurdle that prevents complete alignment at low temperatures and/or for small fields. Results indicate the molten composite is a non-Newtonian fluid that can support a yielding stress. Scanning Electron microscopy (SEM) images taken on field-annealed samples at 230 °C show strong chaining with little PA-12 left between individual Sr-ferrite particles suggesting that direct particle to particle interaction is the reason for the observed non-zero yielding stress. The melt viscosity of the composite increases with the number of thermal cycles above the melting temperature (T<sub>m</sub>). Room temperature (RT) torque magnetometry measurements show that magnetic anisotropy depends on the field annealing process through induced shape anisotropy contributions originating from magnetic particle agglomerates.

© 2023 Author(s). All article content, except where otherwise noted, is licensed under a Creative Commons Attribution (CC BY) license (http://creativecommons.org/licenses/by/4.0/). https://doi.org/10.1063/9.0000596

#### I. INTRODUCTION

Magnetic Field Assisted Additive Manufacturing (MFAAM), or 3D printing in a magnetic field, is a new manufacturing method that allows for the realization of new materials and devices whose magnetic anisotropy axis varies as a function of position. Such materials cannot yet be made by any other manufacturing method. Applications of hard magnetic MFAAM materials include Halbach cylinders for use in energy efficient electromotors and generators and high-performance permanent magnets for use for example in portable MRI equipment. In addition, these new MFAAM materials might replace magnetic polymer composites applied in rapid prototyping or high-performance applications. Properties of such magnetic composites depend on the particle microstructural distribution within the polymer matrix<sup>1</sup> At elevated temperatures, above the softening temperature of the polymer matrix but below the Curie temperature of the single domain magnetic particles, the polymer matrix loses its ability to fix the orientation of the non-spherical magnetic particles and individual particles rotate freely, lining up with an externally applied field.<sup>2</sup> This alignment process influences the distribution pattern of the magnetic particles in the suspension. The particles attract each other due to the magnetic force

originating from the magnetostatic interaction, and eventually organize in long chains parallel to the direction of the applied magnetic field.3 This interaction and chaining process is enhanced in suspensions exposed to a magnetic field. So, two effects are observed: (1) the alignment of the magnetic particles due to the rotation inside the molten matrix towards an externally applied magnetic field and (2) the redistribution of the aligned magnetic particles due to the inhomogeneous magnetostatic interaction field often referred to as magnetic chaining.<sup>2–8</sup> If the matrix is cooled down to room temperature in a field, the frozen-in magnetic texture and chain morphology make the composite anisotropic. Here, we report on the magnetic anisotropy of 5 and 40 wt. % SrO(Fe<sub>2</sub>O<sub>3</sub>)<sub>6</sub>/PA-12 composites (read 1 vol. % and 8 vol. %) after field-anneals above T<sub>m</sub>. The rotation of magnetic dipoles during the field annealing process above T<sub>m</sub> is studied with a biaxial VSM using a similar method as described in Ref. 2. The chaining is studied through direct SEM studies on field-annealed samples.

#### II. EXPERIMENTAL PROCEDURE

OP-71 Strontium Ferrite [SrO(Fe<sub>2</sub>O<sub>3</sub>)<sub>6</sub>] powder obtained from Dowa Electronics Materials Corporation and Vestosint® 3D Z2773 PA-12 (Nylon) ( $T_m \sim 178$   $^{\circ}C^{9}$ ) from Evonik were used to realize 5 and 40 wt. % SrO(Fe<sub>2</sub>O<sub>3</sub>)<sub>6</sub>/PA-12 composite 3D printer filaments. OP-71 powder consists of strontium ferrite platelets (Curie temperature is 477 °C) with an average diameter of 1.39 μm. SEM images of the as-received powder reveal a large spread in diameter i.e. 0.1-4.5 µm. Individual particles are platelets with a typical aspect ratio of 3. These particles do not have a perfect hexagonal shape suggesting they are polycrystalline but have a strong texture. 10 Using the Ms and K data of Ref. 11 the calculated RT single domain size of strontium ferrite is approximately 0.6  $\mu$ m and increases to 1.2  $\mu$ m at 230 °C, the field-anneal temperature used in this paper. Although these values suggest that the largest particles are multidomain the coercivity of both studied composites is close to 4 kOe. A Thermo Fisher Process 11 co-rotating twin-screw extruder was used to manufacture the magnetic polymer composite filaments. 12,1 The particle's orientation and distribution in the filaments was studied with a FEI Helios NanoLab 400 DualBeam SEM. Samples were cut at RT perpendicular to the cylindrical axis using a surgical knife. All samples were coated with a conductive 4 to 6 nm layer of Iridium (Ir) deposited by a Quorum Technologies EMS150T Imaging Sputter Coater. The 5 wt. % filaments needed a thicker coating (6 nm) to avoid charging issues than the 40 wt. % filaments (4 nm) that have a higher loading level.2

The field-anneal, the magnetic rotation studies, and the torque measurements were all done using a MicroSense-KLA biaxial EZ-9 VSM furnished with a 70–1000 K temperature option flowing Argon (Ar) gas at 230 °C. This temperature (230 °C) was chosen to simulate the alignment of the particles during the 3D printing process as it is in the center of the process 3D-print window defined by PA-12's  $T_{\rm m}~(175\,^{\circ}{\rm C})$  and the onset of decomposition of the Nylon matrix (290–400 °C).  $^{14}$  Note that, up to 290 °C the weight loss observed in TGA graphs is negligible.

Samples were 4–6 mm long cylindrical filaments with an average diameter of 1.5 mm and typically had a mass of around  $\sim$ 14 mg. The sample's mass was measured with a C-30 Cahn microbalance that has a resolution down to 1 microgram. They were loaded in

a Pyrex glass tube with an outer diameter of 3 mm and an inner diameter of 1.75 mm [Fig. 1(a)]. The filament was wrapped with Teflon plumber tape that has a low surface free energy to avoid the composite to wet with the Pyrex tube upon melting and turn into a hollow cylinder at 230 °C [Fig. 1(b)]. PEEK stoppers with high temperature silicone glue on both sides of the samples were used to secure the sample's position and prevent the molten composite to leak out the glass rod. The VSM's furnace was used to heat up the sample for the field-anneal and the rotation studies. This furnace operates under Ar and allows temperature rates up to  $1.1\,^{\circ}\text{C/s}$ .

The rotation of the magnetic particles in the molten suspension was studied with the biaxial VSM. Filament samples were annealed in a field of 22 kOe at 230 °C for 3 min and cooled down in a magnetic field. Then the sample was rotated in zero field over 90 degree to orient its magnetic dipole moment perpendicular to the field direction. A step field of 500 Oe was applied to exert a torque on the magnetic particles that rotates them towards the field direction. Please note that the applied field is much smaller than the coercivity and anisotropy field so thus not significantly affects the particle's magnetic dipole moment which is expected to line up close to the particle's easy axis. During the application of this field, the sample's  $M_x$  and  $M_y$  components were recorded to monitor the rotation of the particles in the nylon matrix through  $\theta(t)=\tan^{-1}$  $(M_v(t)/M_x(t))$ . This experiment was repeated for different temperatures on the same sample to explore how temperature affects the alignment process. More details on this novel method can be found in Ref. 2.

Torque measurements have been widely used to measure a sample's magnetic anisotropy.<sup>15</sup> One measures the torque exerted as a function of the field angle and magnitude, and the magnetic anisotropy is determined from an inverse Fourier series analysis of the torque curve. Although usually torque magnetometers are used, one can also indirectly measure torque with a biaxial VSM from the components of magnetic moment perpendicular to the field direction since:

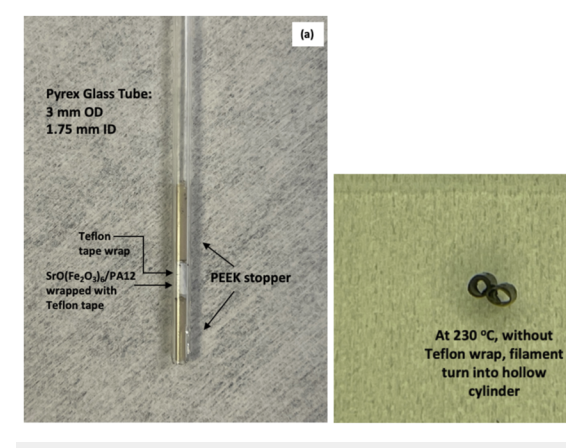


**FIG. 1.** (a)  $SrO(Fe_2O_3)_6/PA12$  cylindrical-shaped filament wrapped with Teflon tape and secured in Pyrex glass tubes with PEEK stoppers and high temperature silicone glue (b) at  $230\,^{\circ}C$  upon melting, without Teflon wrap, filament turn into hollow cylinder.

(b)

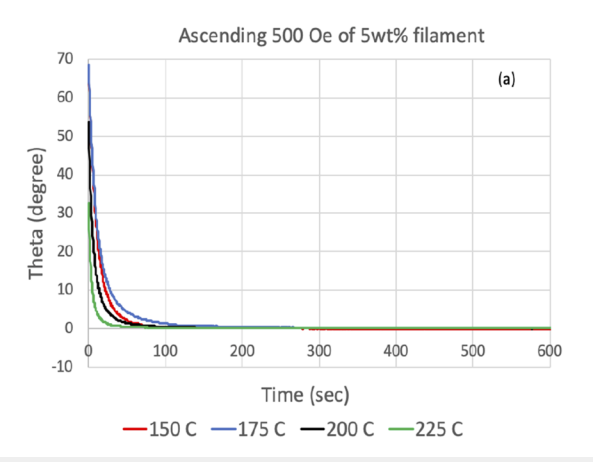
$$\tau = \mu_o \mathbf{M} \times \mathbf{H} = \mu_o M_v H_x \widehat{e}_z + \mu_o M_z H_x \widehat{e}_v$$

where  $M_y$  and  $M_z$  are the components of the magnetic dipole moment perpendicular to the applied field  $H_x$ .<sup>16</sup>

Torque measurements were done at RT using the biaxial VSM on one-time annealed samples in a field of 1.5 kOe for 1, 5 and 180 s. Additional torque measurements were done on samples annealed for 180 s at 230 °C in zero field (zero-field-sample) and in 22 kOe (22 kOe-sample). Prior to the torque measurements the samples were centered in between the X-pickup coils at zero field angle. Torque curves were measured in steps of 10 degrees for different field values from 10 to 22 kOe with field increments of 2 kOe. The torque was determined from the y-intersect of the  $1/H_a - \tau$  curve and converted to magnetic anisotropy by dividing the torque by the volume of the strontium ferrite in the sample calculated from the sample's mass, packing fraction and densities of Nylon ( $\rho$ =1 gr/cm³) and hexaferrite ( $\rho$ =5.18 gr/cm³).

#### **III. MEASUREMENT RESULTS**

Figures 2 and 3 show the time dependence of the magnetic moment angle of 5 and 40 wt. % filament samples under exposure of a 500 Oe field step perpendicular to the field-anneal direction for different temperatures. All measurements were done on the same samples and in between each curve the sample was field-annealed along the same direction using the recipe mentioned in Sec. II. The ascending series in Figs. 2(a) and 3(a) show the first four scans (150 °C, 175 °C, 200 °C, 225 °C) done on respectively the 5 and 40 wt. % sample. Figures 2(b) and 3(b) show the next four scans (225 °C, 200 °C, 175 °C, 150 °C) on respectively the 5 and 40 wt. % sample. The observed transients depend on the temperature similar to what was observed in a previous study for field-anneals below the  $T_m$ .<sup>2</sup> The initial slope of the transients  $\left(\frac{d\theta}{dt}\Big|_{t=0}\right)$  increases with temperature and the limiting magnetic moment angle at large t,  $[\theta(600)]$ , decreases with temperature. The transients depend strongly on the packing fraction (Figs. 2 and 3) with the initial slopes for the high



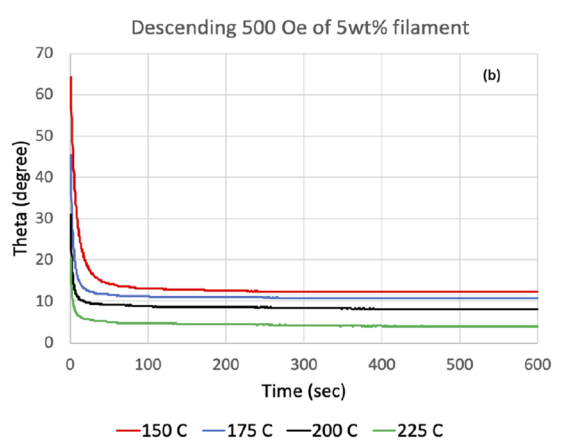
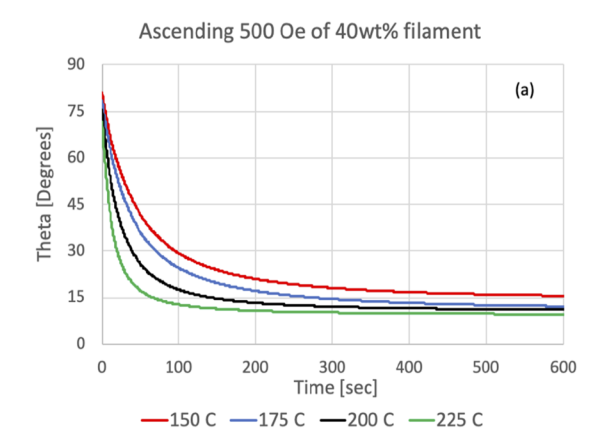


FIG. 2. Magnetic transient upon application of a 500 Oe field perpendicular to the easy axis of 5 wt. % 22 kOe field-annealed at 230 °C composite (a) ascending temperature from 150 to 225 °C (left); (b) descending 225 °C to 150 °C (right).



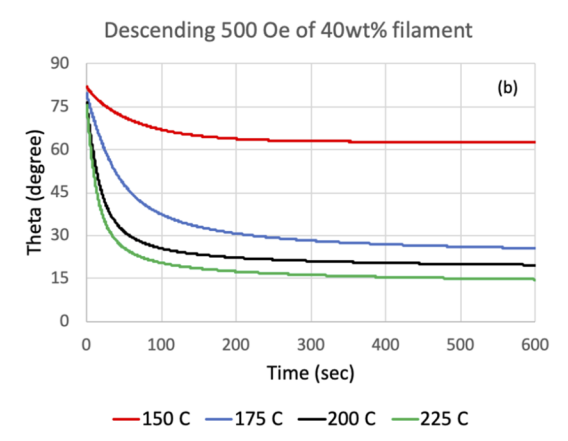


FIG. 3. Magnetic transient upon application of a 500 Oe field perpendicular to the easy axis of 40 wt. % 22 kOe field-annealed at 230 °C composite (a) ascending temperature from 150 to 225 °C (left); (b) descending 225 °C to 150 °C (right).

packing fraction samples a factor 4 to 20 smaller indicating an increase of viscosity with packing fraction as also is observed in other composites.  $^{17}$  Viscosity increases with multiple thermal cycles above  $T_m$  as seen in Figs. 2 and 3 are consistent with what other people found for PA-12.  $^{17,18}$  Strong particle to particle interaction in particularly for the 40 wt. % samples is shown by the large  $\theta(600)$ . In particularly after several field-anneal cycles the  $\theta(600)$  increases (Fig. 3). It is clear from this data that the molten composite (200 and 225 °C curves) is a non-Newtonian fluid that can support a yielding stress and that the strength of this yielding stress shows hysteresis, depends strongly on the packing fraction and is affected by the number of high temperature field-anneal cycles the sample is exposed to.

The SEM images of 5 and 40 wt. % SrO(Fe<sub>2</sub>O<sub>3</sub>)<sub>6</sub>/PA12 pristine filaments are shown in Figs. 4(a) and 4(b), respectively. Very little agglomeration or grouping is observed in the as-extruded samples. Apparently forces originating from the shear flow in the extrusion die and/or the rotation of the extrusion screws compete with the magnetostatic interaction forces and keep the particles apart in the pristine filament. Note that the orientation and possible concentration of the platelets along the r-direction of the filament is expected to be inhomogeneous due to the shear flow in the extrusion die as shown by others. 19,20 VSM hysteresis curve measurements show that the as-extruded filament has a weak c-axis magnetic texture along the filament's r-direction originating from flow induced anisotropy. 12

Figure 5 above shows the effect of field-annealing at 230 °C on the agglomeration of the magnetic particles. These SEM micrographs depicts that, there is considerable amount of agglomeration occurring in both annealed filaments compared to the pristine filament of Fig. 4.

However, the shape of the agglomerates in the zero field samples is extremely random due to the absence of any applied magnetic field and chains are much shorter compared to the samples annealed in a field. Clear chaining along the applied field direction is observed in the samples field-annealed at 22 kOe. The cluster size is larger for the high packing fraction filament. Individual particles in the chains are randomly oriented in the zero field-annealed filaments. With the increase of the field to 22 kOe, the orientation of the strontium ferrite particles in the chain are more directional along the field direction (c-axis parallel to the field direction). Note that the cluster size is much higher in the 22 kOe field-annealed for both 5 and 40 wt. %

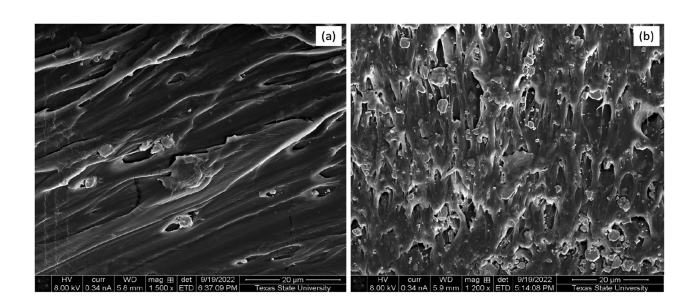
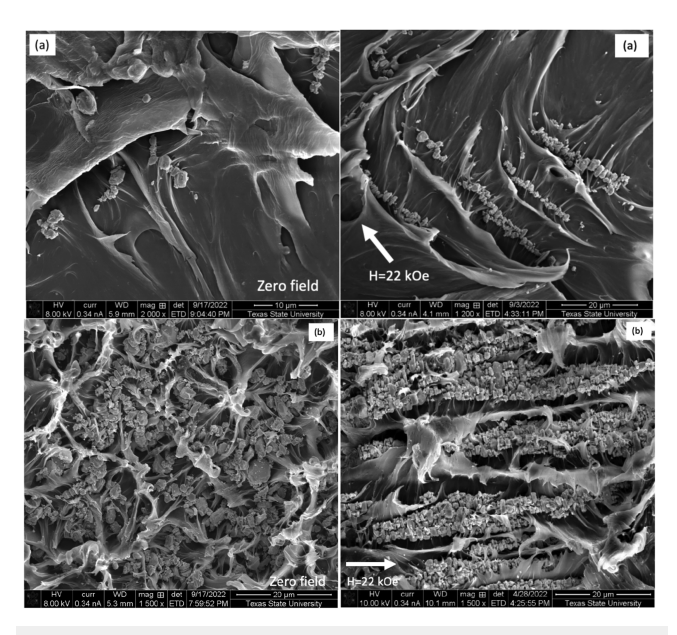


FIG. 4. SEM images of Pristine (a) 5 wt. % and (b) 40 wt. % SrO(Fe $_2\text{O}_3)_6/\text{PA12}$  composite.



**FIG. 5.** Effect of anneal-field on agglomeration: SEM images of zero field and 22 kOe field-annealed at 230  $^{\circ}$ C for 3 min for (a) 5 wt. % (top) and (b) 40 wt. % (bottom) SrO(Fe<sub>2</sub>O<sub>3</sub>)<sub>6</sub>/PA12 filament.

 $SrO(Fe_2O_3)_6/PA12$  composites compared to the zero field-annealed samples.

The effect of the annealing time on the agglomeration and orientation is shown in Fig. 6. These SEM micrographs depict that, there is a considerable amount of chaining formation and particle rotation occurring for anneal-fields lower than 22 kOe. For these smaller fields the magnetic chaining is still more or less along the

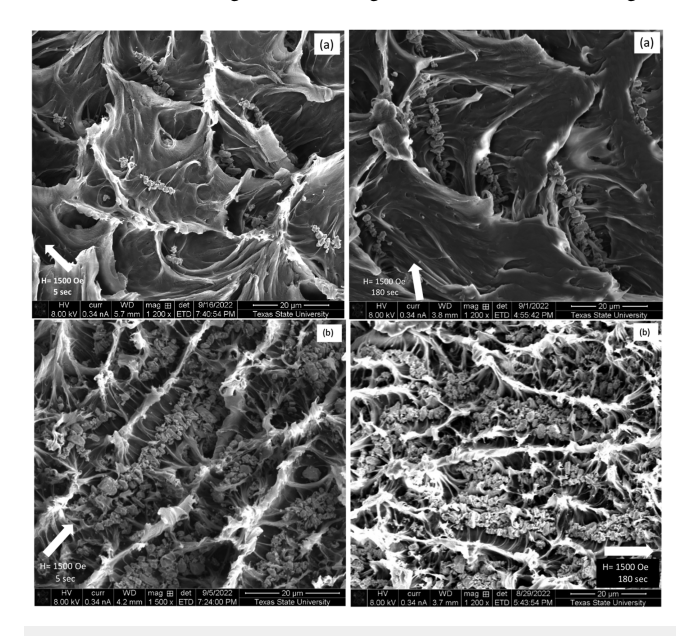


**FIG. 6.** Effect of anneal-time on agglomeration: SEM images of 1500 Oe field-annealed at 230 °C for 5 s and for 180 s for (a) 5 wt. % (top) and (b) 40 wt. % (bottom)  $SrO(Fe_2O_3)_6/PA12$  filament.

field direction although a larger spread in the chain and individual particle directions are observed. It was additionally observed that, higher field annealing time (180 s) not only controlled particle agglomeration but also improves the degree of particle alignment in the field direction. Hence, there is a clear anneal-time dependence on agglomeration size and orientation distribution.

#### IV. DATA ANALYSIS AND DISCUSSION

The SEM images in the previous section show significant particle agglomeration for all samples except for the pristine filament samples. The cluster size increases with anneal-field, anneal time, and packing fraction and is summarized in Table I below. All three effects are understandable. A large anneal-field results in a strong alignment of the particles' magnetic dipole moments which increases the magnetostatic interaction and the speed with which they chain. Similarly, a larger packing fraction results in particles initially already being closer together in the pristine filament increasing the initial magnetic force the particles exert on each other speeding up the chaining process.<sup>3,21,22</sup> Additionally, longer annealing time allows for particles initially farther apart to chain-up resulting in longer chains. The strong chaining with little PA-12 left between individual Sr-ferrite particles for samples field-annealed at 22 kOe suggests that direct particle to particle interaction should contribute to the observed non-zero yielding stress shown in Figs. 2

The results of the torque measurements are summarized in Table I above. Note that the  $K_{eff}$  of the zero-field samples is not zero but approximately 3% of the magnetic anisotropy observed on the 22 kOe field-annealed samples. We believe that, this is a systematic measurement error originating from a circular trajectory the sample describes as the field angle is rotated through 360 degrees because of small misalignments of the sample on the sample rod. It has been recently shown that such trajectory results in a 20 background signal in the Y-coils caused by the angular dependent cross talk term, i.e.  $S_{xy}(\theta)^* M_x$ . Although it is possible to subtract this background

signal, it is small compared to the magnetic anisotropy signal of the field-annealed samples and can be ignored for the discussion below.

 $K_{eff}$  increases with annealing time and annealing field. In addition to the crystal anisotropy and texture  $K_{eff}$  has three contributions due to shape, i.e. the shape of the individual particles, the shape of the agglomerates and the shape of the sample.  $^{24}$  As anisotropy measurements were made in a plane perpendicular to the filament's cylindrical axis and the samples are rotation symmetric along their vertical cylindrical axes, we do not expect any contributions from the sample's macroscopic shape on the measured torque curves. When the strontium ferrite particles are far apart and do not interact at all, are single crystalline, and all of them are oriented in the same direction, the total magnetic anisotropy,  $K_{\rm eff}$ , will be:

$$K_{eff} = K_{cr} - \frac{1}{2}\mu_o N_d M_s^2$$

Where  $K_{cr}$  is the crystal anisotropy of strontium ferrite which is 350 kJ/m³25 and the 2nd term is the shape anisotropy of individual particles. For particles with an aspect ratio of 3 (OP-71), Nd is 0.64 and  $K_{\rm eff} = 309$  kJ/m³. If the particles are not perfectly aligned or are not single crystalline the effective  $K_{\rm eff}$  will be lower. Assuming  $N_{\rm d}$  is correct, a  $K_{\rm eff} > 309$  kJ/m³ indicates the particles are chained along the anneal field direction and interact with each other. As the samples annealed in 22 kOe have an effective anisotropy beyond 350 kJ/m³ (see Table I) the torque measurements provide proof of chaining. The samples annealed at lower fields show all an effective anisotropy below 309 kJ/m³ but still could be chained as additional shape anisotropy of the elongated agglomerates could be canceled by the poor alignment of the individual particles.

The large value of the measured  $K_{\rm eff}$  depends on the field annealing process through induced shape anisotropy contributions originating from the shape anisotropy of the particles and the directional agglomerates. The magnetic anisotropy increases with increase of the field annealing time for both 5 and 40 wt.%  $SrO(Fe_2O_3)_6/PA12$  composites.

**TABLE I.** Cluster size and magnetic anisotropy of pristine and 230 °C field-annealed 5 and 40 wt. % composite.

SrO(Fe <sub>2</sub> O <sub>3</sub> ) <sub>6</sub> /PA12 composite	Annealing field (Oe)	Annealing time (s)	Avg. cluster size (number)	Anisotropy, K <sub>eff</sub> (kJ/m <sup>3</sup> )
5 wt. %	Pristine		2.5	
	0	0	9.0	12.4
	1500	1		96.7
	1500	5	15.5	104.0
	1500	180	18.9	116.5
	22 000	180	26.7	432.3
40 wt. %	Pristine		4.9	
	0	0	44.0	10.8
	1500	1		172.9
	1500	5	77.0	189.0
	1500	180	102.0	221.1
	22 000	180	169.0	356.1

#### V. CONCLUSIONS

A biaxial VSM was used to study the magnetic anisotropy of the strontium ferrite-PA12 composite induced by field annealing at 230 °C. The magnetic anisotropy depends on the field annealing process through induced shape anisotropy contributions originating from agglomerates. It increases with increase of the field annealing time for both 5 and 40 wt. % SrO(Fe<sub>2</sub>O<sub>3</sub>)<sub>6</sub>/PA12 composites. For 22 kOe field-anneals, the measured magnetic anisotropy is larger than an individual particle's Keff, providing evidence for significant agglomeration along the anneal field direction. This conclusion is supported by SEM analysis showing good particle alignment and significant chaining. Cluster size determined from SEM analysis and magnetic anisotropy determined from torque measurements on samples field-annealed at lower fields are correlated and increase with anneal field, anneal time, and packing fraction. Biaxial VSM was also used to monitor the rotation of the magnetic moment in field-annealed samples exposed to a small field perpendicular to the field-anneal direction. The rotation time constant, which is inversely proportional to the viscosity, decreases with temperature. At lower temperatures and smaller rotation fields, it is not possible to align the sample's magnetic dipole moment up with the rotation field direction. SEM images suggest that strong chaining limits the space available for the non-spherical particles to rotate over a full 90 degrees and is responsible for the observed non-zero yielding strength. The latter increases with packing fraction which indicates that the required MFAAM alignment fields resulting in decent alignment also increases with packing fraction. To further the development of MFAAM a model of the MFAAM deposition process<sup>26</sup> that also includes chaining processes<sup>27</sup> needs to be developed to better understand how viscosity and packing fraction affect non-spherical particle alignment processes.

Lastly, it was observed that viscosity and yielding strength increase when the composite is exposed to multiple thermal cycles above  $T_{\rm m}$ . PA-12 polymers often contain reactive chain ends and these reactive end groups can react at elevated temperatures, particularly above  $T_{\rm m}$ , to increase molecular weight which has a large effect on viscosity for a linear polymer as shown by others.  $^{17,18}$ 

# **ACKNOWLEDGMENTS**

This work was supported in part by NSF through DMR-MRI Grants under Awards 1726970 and 2216440, in part by DOD through a HBCU/MI grant (W911NF2010298), and in part by a Research Enhancement grant from Texas State University. TA acknowledges scholarship support of the international chapter of the PEO sisterhood and the graduate college of Texas State through dissertation support grant. The authors would also like to acknowledge the help of Dr. Erik Samwel of MicroSense-KLA to implement the modifications to the VSM software to allow for simultaneous monitoring of both  $\rm M_x$  and  $\rm M_y$  versus time.

#### **AUTHOR DECLARATIONS**

#### **Conflict of Interest**

The authors have no conflicts to disclose.

#### **Author Contributions**

Tanjina N. Ahmed: Conceptualization (equal); Data curation (equal); Formal analysis (equal); Investigation (equal); Methodology (equal); Resources (equal); Software (equal); Validation (equal); Visualization (equal); Writing – original draft (equal); Writing – review & editing (equal). Christopher Selsor: Data curation (equal); Methodology (equal). Jitendra S. Tate: Funding acquisition (equal); Project administration (equal); Resources (equal). Wilhelmus J. Geerts: Conceptualization (equal); Funding acquisition (equal); Project administration (equal); Resources (equal); Supervision (equal); Writing – review & editing (equal).

#### **DATA AVAILABILITY**

The data that support the findings of this study are available from the corresponding author upon reasonable request.

#### **REFERENCES**

- <sup>1</sup>B. Nagarajan, M. A. W. Schoen, S. Trudel, A. J. Qureshi, and P. Mertiny, Polymers 12(9), 2143 (2020).
- <sup>2</sup>T. N. Ahmed, C. Belduque, M. Y. Chen, J. S. Tate, and W. J. Geerts, AIP Adv. 12, 095223 (2022).
- <sup>3</sup>H. Wu, Z. Xu, J. Wang, X. Bo, Z. Tang, S. Jiang, and G. Zhang, J. Magn. Mater. **527**, 167693 (2021).
- <sup>4</sup>J. J. Romero, R. Cuadrado, E. Pina, A. de Hoyos. F. Pigazo, F. J. Palomares, A. Hernando, R. Sastre, and J. M. Gonzalez, J. of App. Phys. **99**(8), 08N303 (2006).
- <sup>5</sup>J. E. Martin, E. Venturini, J. Odinek, and R. A. Anderson, Phys. Rev. E Stat. Physics, Plasmas, Fluids, Relat. Interdiscip. Top. 61(3), 2818–2830 (2000).
- <sup>6</sup>E. Joven, A. Del Moral, and J. I. Arnaudas, J. of Magn. and Mag. Mater. **83**, 548 (1990).
- <sup>7</sup>R. M. Erb, J. Segmehl, M. Charilaou, J. F. Löffler, and A. R. Studart, Soft Matter 8(29), 7604–7609 (2012).
- <sup>8</sup>D. Kokkinis, M. Schaffner, and A. R. Studart, Nat. Commun. 6, 8643 (2015).
- <sup>9</sup>G. V. Salmoria, J. L. Leite, L. F. Vieira, A. T. N. Pires, and C. R. M. Roesler, Polym. Test. 31(3), 411–416 (2012).
- <sup>10</sup>M. Camila Belduque Correa, "Development of strontium ferrite/polyamide 12 composites for magnetic devices using additive manufacturing," M.S. thesis, Texas State University, 2021.
- <sup>11</sup>B. T. Shirk and W. R. Buessem, J. Appl. Phys. **40**, 1294–1296 (1969).
- <sup>12</sup>T. N. Ahmed, M. C. Belduque, D. C. Binod, J. S. Tate, and W. J. Geerts, AIP Adv. 11, 015048 (2021).
- <sup>13</sup>C. Belduque, R. Robinson, A. Medina, T. Ahmed, R. Kala, W. Geerts, and J. Tate, in Society for the Advancement of Material and Process Engineering, Long Beach, CA, 24–27 May 2021 (SAMPE, 2021), p. 686.
- <sup>14</sup>S. V. Levchik, E. D. Weil, and M. Lewin, Polym. Int. **48**(7), 532–557 (1999).
- <sup>15</sup>B. D. Culity and C. D. Graham, "Magnetic anisotropy," in *Introduction to Magnetic Materials*, 2nd ed. (Wiley-IEEE Press, 2008), ISBN: 9780471477419, Chap. 7
- <sup>16</sup>B. C. Dodrill, J. R. Lindemuth, and J. K. Krause, Lake Shore Cryotronics Inc., 575 McCorkle Blvd., Westerville, OH, USA.
- <sup>17</sup> J. Bai, R. D. Goodridge, R. J. M. Hague, M. Song, and M. Okamoto, Polym. Test. 36, 95–100 (2014)
- <sup>18</sup>G. M. Craft, "Characterization of nylon-12 in a novel additive manufacturing technology, and the rheological and spectroscopic analysis of PEG-starch matrix interactions," Ph.D. dissertaion (University of South Florida, 2018).
- <sup>19</sup>B. P. Heller, D. E. Smith, and D. A. Jack, Addit. Manuf. **12**, 252–264 (2016).

<sup>20</sup> J. H. Phelps and C. L. Tucker, J. Non-Newton. Fluid Mech. **156**, 165–176 (2009).

- $^{\mathbf{24}}$ R. Skomski, G. C. Hadjipanayis, and D. J. Sellmyer, IEEE Trans. Magn.  $\mathbf{43}(6)$ , 2956–2958 (2007).
- <sup>25</sup> A. Z. Eikeland, M. Stingaciu, A. H. Mamakhel, M. Saura-Múzquiz, and M. Christensen, Sci. Rep. 8(1), 7325 (2018).
- <sup>26</sup> A. Sarkar, M. P. Paranthaman, and I. C. Nlebedim, Addit. Manuf. 46, 102096 (2021).
- <sup>27</sup>S. A. Faroughi and C. Huber, Rheol. Acta **56**(1), 35–49 (2017).

<sup>&</sup>lt;sup>21</sup> J. G. Ku, X. Y. Liu, H. H. Chen, R. D. Deng, and Q. X. Yan, AIP Adv. **6**(2), 025004 (2016).

<sup>&</sup>lt;sup>22</sup>B. F. Edwards and J. M. Edwards, Eur. J. Phys. 38(1), 015205 (2017).

<sup>&</sup>lt;sup>23</sup>K. J. Dieckow, "Automatic alignment methods for VSM usibg magnetic low anisotropic samples with reduced time and higher precision," M.S. thesis, Texas State University, 2021.